Biosensors and Bioelectronics 224 (2023) 115014

Contents lists available at ScienceDirect

Biosensors and Bioelectronics

journal homepage: www.elsevier.com/locate/bios

Aptamer-functionalized capacitive biosensors

Sean Weaver, Melika Haji Mohammadi, Nako Nakatsuka *

Laboratory of Biosensors and Bioelectronics, Institute for Biomedical Engineering, ETH Zürich, CH-8092, Switzerland

ARTICLE INFO

Keywords:
DNA
RNA
Conformational change
Non-faradaic
Label-free
Impedance

ABSTRACT

The growing use of aptamers as target recognition elements in label-free biosensing necessitates corresponding transducers that can be used in relevant environments. While popular in many fields, capacitive sensors have seen relatively little, but growing use in conjunction with aptamers for sensing diverse targets. Few reports have shown physiologically relevant sensitivity in laboratory conditions and a cohesive picture on how target capture modifies the measured capacitance has been lacking. In this review, we assess the current state of the field in three areas: small molecule, protein, and cell sensing. We critically analyze the proposed hypotheses on how aptamer-target capture modifies the capacitance, as many mechanistic postulations appear to conflict between published works. As the field matures, we encourage future works to investigate individual aptamer-target interactions and to interrogate the physical mechanisms leading to measured changes in capacitance. To this point, we provide recommendations on best practices for developing aptasensors with a particular focus on considerations for biosensing in clinical settings.

1. Introduction

To date, approximately 30 manuscripts have been published on capacitive aptamer sensors (aptasensors). Capacitive sensors are an attractive label-free method for many biosensing applications due to their high sensitivity, relatively simple readout electronics, and potential scalability (Santos et al., 2015; Tsouti et al., 2011; Berggren et al., 2001). Aptamers are single-stranded, short oligonucleotides (typically <100 nucleotides) serving as artificial molecular recognition elements for specific targets of interest (Zhou and Rossi, 2016). While there has been success applying capacitive measurements for the detection of various analytes of interest, in general, an in-depth understanding of the physics/chemistry is lacking across the published works. Further, we have observed conflicting hypothesized mechanisms within the capacitive aptasensing literature.

For this technology to mature, a deeper understanding of the nature of capacitance in these systems is necessary. Comprehending this phenomenon is challenging, especially with the variation in target molecules, aptamer sequences, aptamer-target binding mechanisms, and capacitor electrode size and dimensions. Nevertheless, we attempt to provide some insight by reviewing the existing literature critically and emphasize the necessity to perform comprehensive characterizations of individual aptamer-modified capacitive biosensors.

Introducing aptamers on the surface of electrodes clearly modifies the thickness, charging, and total charge of the electrical double layer (EDL) as well as the effective permittivity of the solution. These properties are further modified when aptamers bind specific targets of interest in sequence-specific mechanisms. When capacitance measurements are made in complex solutions at voltages above the thermal potential (~25 mV at 20°C) or at high frequencies, many equivalent circuit models are insufficient (Kilic et al., 2007). In this review, we first introduce the field of aptamers as molecular recognition elements, then describe the existing literature in capacitive aptasensing while evaluating the variability in mechanistic hypotheses. Finally, we summarize key points that should be taken into careful consideration in the design and testing of capacitive aptasensors for clinical applications.

2. Aptamers as molecular recognition elements for biosensing

Not all single-stranded oligonucleotides bind to a target of interest selectively, this instead, is the defining feature of aptamers, which are isolated by an *in vitro* combinatorial method termed systematic evolution of ligands through exponential enrichment (SELEX) (Ellington and Szostak, 1990; Tuerk and Gold, 1990). This approach circumvents *de novo* design necessary for more conventional protein-based recognition elements such as enzymes and antibodies. Aptamers targeting diverse

Abbreviations: Aptasensor, aptamer sensor; EDL, electrical double layer; SELEX, systematic evolution of ligands by exponential enrichment.

* Corresponding author.
E-mail address: nakatsuka@biomed.ee.ethz.ch (N. Nakatsuka).

https://doi.org/10.1016/j.bios.2022.115014
Received 16 September 2022; Received in revised form 17 November 2022; Accepted 13 December 2022
Available online 23 December 2022

biomolecules ranging from small molecules to large proteins and cells (*via* recognition of specific ligands on cell membranes) have been reported (Darmostuk et al., 2015). Further, advances in SELEX have facilitated the identification of specific and selective aptamers for challenging targets (Yang et al., 2012, 2014, 2017). Aptamer specificity is defined as target recognition with adequate affinity while selectivity refers to the ability to discriminate structurally similar analytes found in comparable concentrations in the sensing environment. Such characteristics facilitate the deployment of aptamers for a variety of applications including biomedical diagnostics, biomarker discovery, and targeted therapies (Zhou and Rossi, 2016).

The appeal of aptamers lies in minimal batch-to-batch variation and low production costs due to chemical synthesis of relatively short sequences (Baker, 2015). Further, aptamers can be chemically stabilized *via* conjugation to carrier molecules, such as polyethylene glycol, or capped at their 3'- and/or 5'-ends to enhance nuclease resistance for deployment in biological media (Ni et al., 2017). Being artificial, aptamers can be tuned by manipulating primary base sequences to control folding kinetics and binding affinities (Ricci et al., 2016; Bissonnette et al., 2020). The selectivity of aptamers for specific applications in biological milieu with high concentrations of nonspecific interferents can be optimized *via* improved SELEX procedures. Counter-SELEX or negative selection excludes sequences with high affinity for cross-reactive targets and thus improves aptamer selectivity towards molecules of interest *vs.* structurally similar nontargets (Yang et al., 2012, 2014).

A critical aspect of aptasensing relies on the mechanism of detection. However, the mechanism is target dependent, where binding of large, highly charged biomolecules to surface-tethered aptamers alters the surface properties of sensing areas. Instead, for small molecules with single to a few charges or neutral molecules, the binding of the target itself may be insufficient to induce a change in capacitance, especially in low amounts. As an alternative to reducing capacitor dimensions to the nanoscale (Yi et al., 2005; Mannoor et al., 2010; Ghobaei Namhil et al., 2019), aptamers undergoing conformational rearrangement upon target recognition can be harnessed to achieve sensitive neutral and small-molecule sensing (Nakatsuka et al., 2018a).

Especially in diagnostic electronic biosensing where the sensor must be deployed in complex environments such as biofluids or clinical samples, structure-switching aptamers are advantageous (Nakatsuka et al., 2021a). Many real samples have high ionic content leading to a limited effective sensing regime within the screening distance (Debye length) for charge carriers in the solution (Nakatsuka et al., 2018a). Covalent assembly of aptamers on the electrode alters the surface charge due to the highly negatively charged phosphodiester backbone rearranging solution ions in close proximity. Upon target recognition, structural changes driven by intermolecular interactions such as van der Waals forces, pi-pi stacking of bases, and hydrogen-bonding, lead to modulation of charge density near or within the Debye length at sensor surfaces. While a new electrochemical equilibrium will form, often the thermodynamically minimal state allows for uncompensated charge in the volume around the aptamer.

Whether this effect has noticeable impact on charge stored by the electrode depends on aptamer packing and length, buffer concentration, electrode potential, and applied frequency among other parameters. Fig. 1a shows a schematic of the double layer formation on a negatively charged electrode when i) the surface is uncoated ii) a self-assembled monolayer of short backfill molecules (*e.g.,* 6-mercaptohexanol, MCH) are covalently attached to the surface iii) aptamers are co-assembled with backfill molecules and iv) the aptamer undergoes structure switching due to target capture. Importantly, this mechanism of target detection does not require labels such as redox reporters or fluorescent dyes and does not rely on properties of the target molecule (*e.g.,* size, charge, redox potentials). Conformational rearrangements of aptamers can be validated through various complementary techniques such as fluorescence-based strategies (*e.g.,* Förster resonance energy transfer) and spectroscopic methods (*e.g.,* circular dichroism and surface-enhanced Raman spectroscopy) (Bottari et al., 2020).

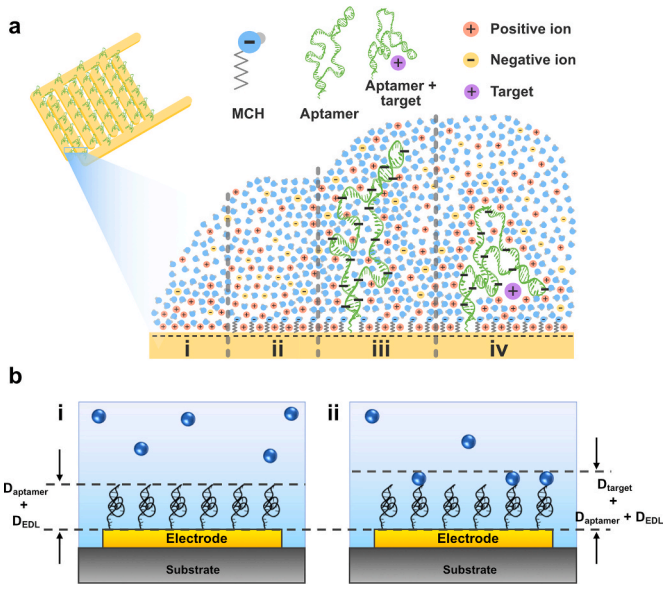

Fig. 1. Mechanisms of detection for capacitive aptasensors. a) Schematic of the double layer for (i) a bare metal surface where a compact layer of counter ions forms, (ii) small backfill molecules (6-mercaptohexanol, MCH) covalently modified on the electrode surface, (iii) negatively charged DNA aptamers assembled alongside the MCH backfill, and (iv) an aptamer that undergoes conformational rearrangements upon target capture. b) Schematic demonstrating the mechanistic hypothesis of changes in interface capacitance upon aptamers binding to targets. (i) The dielectric layer on the electrode surface is composed of the thickness of the electrical double layer (EDL) and the assembled aptamers. (ii) Binding of the target analytes result in an increase in the hight of the dielectric layer.

However, many aptamers do *not* undergo significant structural rearrangements, but rather, similarly to antibodies, have binding pockets that may exist in distant locations from the sensing surface (Orava et al., 2010). Most reports reviewed herein, assume this lock-and-key binding mechanism while neglecting the characterization of specific aptamers with their targets. In this case, the primary mechanism of detection is a change in the effective thickness of the double layer as shown in Fig. 1b. Care must be taken in determining what aptamers to integrate into which capacitive platform, depending on the target of interest and recognition mechanism. Further, the real-world application of the sensor must be taken into consideration, as aptamers adopt different conformational structures with target-binding affinities dependent on the sensing environment (Nakatsuka et al., 2021b; Špringer et al., 2010). With these important aspects of aptasensing in mind, we delve into the existing literature of capacitive aptasensing platforms for various targets ranging from small molecules to whole cells.

3. Capacitive aptasensors

When searching the literature with aptamers integrated as recognition elements in capacitive biosensing platforms, the most common targets are large biomolecules (Fig. 2). The preference for detecting large targets is due to greater changes in charge redistribution on the electrode surface upon binding of highly charged, large biomolecules. Alternatively, there are few studies that targeted small molecules (<0.5 kDa), which are mainly of environmental concern. While occasionally, peptides used for molecular recognition are also called aptamers (Reverdatto et al., 2015; Chand et al., 2016) we report solely on oligonucleotide-based aptamers. Further, we focus our review on capacitive aptasensors.

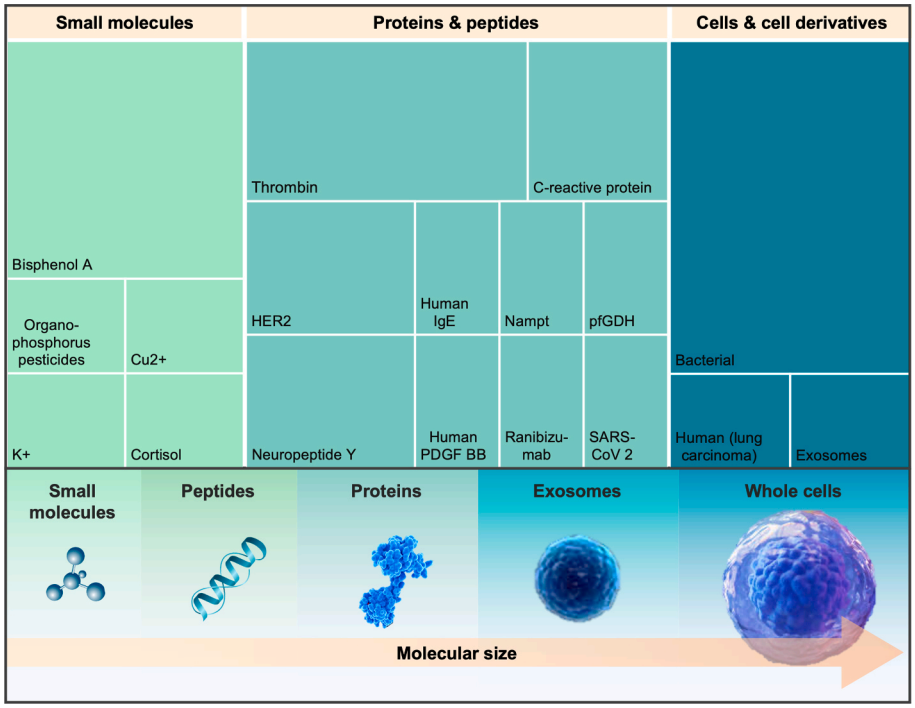

Fig. 2. Distribution of published literature on capacitive aptasensors categorized based on their targets in a tree map. The molecular size differences are illustrated below.

Fundamentally, capacitance is defined as the amount of charge stored on an electrode at a given potential. Capacitance changes in electrochemical sensors can be divided between three phenomena: polarization, EDL capacitance, and pseudocapacitance. While traditionally, pseudocapacitance and EDL capacitance have been considered separate, the physical distinction between the two is not always well defined (Fleischmann et al., 2020). Herein, we review reports involving mechanisms of polarization and EDL capacitance. Pseudocapacitive effects are typically better described by Faradaic charge transfer between the electrodes and the solution and as such, are not addressed here. An overview of redox-mediated and pseudocapacitive aptasensors can be found in a recently published book on aptamers in biotechnology (Urmann and Walter, 2020). Each category of target molecules requires different considerations due to variations in how the aptamer-target interaction influences signal transduction at the surface of capacitive platforms. We will begin by addressing examples of each.

3.1. Small molecules

When reviewing the literature for small-molecule detection using capacitive aptasensors, the trend was a *decrease* in capacitance upon binding of the analyte to the aptamer-modified electrodes. Suggested mechanisms for capacitance decrease include increasing the thickness of the dielectric layer upon target binding to the aptamer-modified electrodes or aptamer conformational change (albeit, without characterization of the dynamics of target-induced structure switching). Analysis of the existing literature of capacitive aptasensors targeting small molecules demonstrates a need to bridge the gap between the fundamental characterization of aptamer-target interactions and electrical aptasensor responses.

Most reported capacitive aptasensors targeting small molecules have been developed to detect toxic chemicals in environmental resources or food. Widespread use of various chemicals in different stages of the food chain has caused concern as some of those chemicals are toxic at low concentrations (Rather et al., 2017). For example, organophosphorus pesticides are widely used in agriculture due to being efficient and cost-effective, but they can cause severe diseases in humans (Eddleston et al., 2008). Zhang *et al.* used a capacitive sensing platform to detect four different organophosphorus pesticides (profenofos, isocarbophos, omethoate, and phorate) simultaneously using an aptamer that can bind to all four targets (Zhang et al., 2020). However, we note that a sequence that binds to four molecules without differentiation, is not a characteristic "aptamer", but rather a sequence with cross-reactivity to multiple targets (Álvarez-Martos and Ferapontova, 2017). In this work, the authors characterize the dielectric layer on the electrode surface as the sum of the thicknesses of the electrical double layer and the immobilized aptamers (Fig. 1bi). Upon binding of organophosphorus molecules to the aptamers, the authors hypothesize the dielectric layer of the electrode surface *increases* due to additional thickness of bound organophosphorus molecules (Fig. 1bii). This increase in dielectric layer leads to a *decrease* in capacitance.

However, without robust characterization of the aptamer-target recognition mechanism, it is challenging to know *how* the dielectric layer of the electrode-buffer interface is altered upon binding. While possible that target binding does indeed increase the aptamer layer thickness due to distal binding pockets or conformational rearrangements resulting in elongation of the complex, it is an oversimplification to assume target binding *always* leads to a thicker charged layer at the surface. Some aptamer-target complexes adopt a more compressed structure compared to the free aptamers (Nakatsuka et al., 2018a). Hence, it is important to interrogate aptamer-target interactions to form models of capacitive aptasensors.

Two research teams fabricated capacitive aptasensors to monitor bisphenol A (BPA), a small molecule commonly used in the production of food/water containers that has been shown to have adverse effects on the mammalian endocrine system at low concentrations (Yoon et al., 2014; Almeida et al., 2018). While Kang *et al.* attributed decrease in capacitance to aptamer conformational change, there was no discussion on *how* the backbone rearrangement upon BPA recognition resulted in lower capacitance (Kang et al., 2011). Cui *et al.* similarly saw capacitance decrease with increasing BPA concentrations but the mechanism was not postulated (Cui et al., 2016). An important factor to consider is that two different aptamer sequences were used with varying sequence lengths (>100 bases for Kang *et al.*, ~60 bases for Cui *et al.*) likely

possessing distinctive binding dynamics upon BPA recognition. To this point, each unique aptamer-capacitive sensor system should be interrogated on a case-by-case basis to decipher the relationship between recorded capacitance changes and aptamer-small-molecule binding.

An alternative report posited aptamer conformational change as the driving mechanism for the detection of potassium ion, K^+. Interestingly, the K^+ aptamer has been characterized in other reports to structure-switch from a random-coil structure to G-quadruplexes with a cavity that fits K^+ ions (Radi and O'Sullivan, 2006; Chen et al., 2013). Formation of the G-quadruplex increases space charge density compared to the random coil due to the significantly decreased DNA persistence length, an indicator for the degree of structural rigidity/flexibility (Radi and O'Sullivan, 2006). For the K^+ aptamer, the persistence length of the condensed G-quadruplex is ~1 nm *vs.* ~6 nm for the random coil despite the same number of negative charges (Zhang et al., 2001; Manning, 1978). Thus, the K^+ aptamer conformational change that alters the thickness and dielectric properties of the sensing layer was believed to modify the interfacial capacitance. While this work used a previously characterized aptamer, since the charge of the aptamer, target, and electrode dimensions influences such measurements, each of these components must be deconstructed for a comprehensive mechanistic understanding.

Especially for small molecules with small charges and low masses, aptamer conformational dynamics that rearranges the highly negative charges at sensor surfaces likely drive the changes observed in measured capacitance. The importance of clarifying aptamer rearrangements upon target recognition has been shown using field-effect transistors (FETs) as electronic signal transduction platforms (Nakatsuka et al., 2018a, 2021b). While we do not cover aptamer-functionalized transistors in this review, the surface charge rearrangement of the double layer measured by FETs can provide insight into how aptamer conformational change will impact interfacial charge storage in capacitive sensors.

On FET surfaces, the detection of two small-molecule neurotransmitters, serotonin and dopamine, with comparable molecular weights and the same charge (one positive charge at physiological pH due to the primary amine), resulted in divergent electronic responses in artificial brain fluid (Nakatsuka et al., 2018a). On one hand, for dopamine aptamer-functionalized FETs, a current *decrease* followed increasing concentrations of dopamine (Fig. 3a). On the other hand, serotonin aptamer-functionalized FETs showed an *increase* in current upon addition of serotonin (Fig. 3b). These measurements suggested that the main mode of signal transduction is the aptamer conformational dynamics upon target recognition that influences the charge distribution at the surface of the FETs (Fig. 3c and d).

This study highlights the importance of interrogating how aptamers interact with small molecules to understand the electronic characteristics observed in the capacitive sensing platforms. Further, insight into aptamer conformational changes can lead to optimal surface design (*e.g.,* tailoring aptamer surface densities and chemistries) to maximize the signal-to-noise ratio between specific and nonspecific binding responses. Complementary fluorescence-based or spectroscopic experiments to elucidate binding mechanisms and structural dynamics should be performed in specific environments mimicking the final application of the sensor (*i.e.,* not in highly diluted buffers or water).

Some reports on small-molecule capacitive aptasensors have claimed femtomolar detection of small-molecule targets but measurements were conducted in diluted buffer conditions, which are not representative of biological samples. In some cases, despite the low detection range tested to generate the dose-response curves, the linear regime did not correspond to physiologically relevant sensing regimes. Additionally, in some dose response curves, only the linear regime is recorded without achieving sensor saturation. Nonspecific binding to surfaces scales linearly with ligand concentrations, thus the saturation regime is important to reach to demonstrate specific binding (Frutiger et al., 2021). It is crucial to ensure the linear regime (with highest sensor sensitivity) is within a clinically relevant range to develop a sensor that can be deployed for real-world applications.

3.2. Peptides and proteins

For targets larger than the small-molecule targets (*i.e.,* >0.5 kDa) covered in the previous section, in addition to the influence of aptamer conformational dynamics, the charge and size of the target molecule likely influence the capacitive sensor responses. The electric permittivity

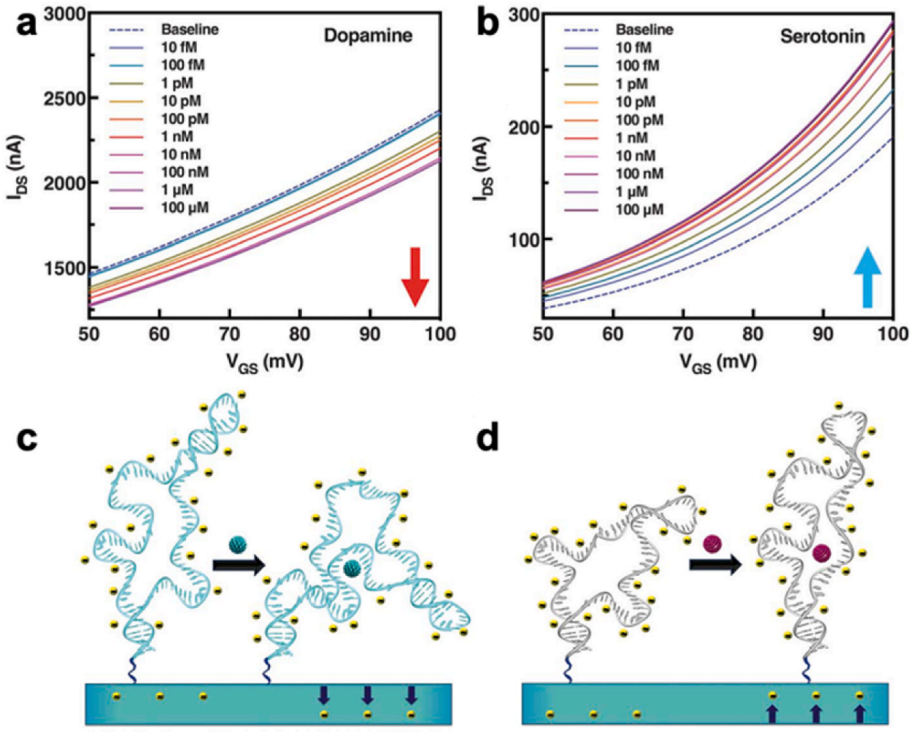

Fig. 3. Divergent electronic signals obtained on the surface of aptamer-modified field-effect transistors (FETs) in artificial cerebrospinal fluid. (a) Exposure of dopamine aptamer-FETs to dopamine led to concentration-dependent decreases in current responses. (b) Alternatively, for serotonin aptamer-FETs, increasing concentrations of serotonin resulted in an increase in current responses. (c) Dopamine aptamers reorient closer to the surface of *n*-type semiconductor FETs, which depletes the channels electrostatically leading to decreases in current responses. (d) Serotonin aptamers structure-switch away from the surface of FETs, which increases the current response, adapted from (Nakatsuka et al., 2018a) Copyright 2018, with permission from the American Association for the Advancement of Sciences.

of the active sensing volume may change substantially when larger targets bind to surface-tethered aptamers and/or the amount of specifically captured charges alters the total charge on the electrode. In some reports that detect peptides and proteins, the charge storage that occurs at the sensor interface is governed by pseudocapacitance rather than double layer capacitance. In some of these scenarios, effective electron transfer reactions (Faradaic) occur at the electrode surface rather than physisorption of ions to form double layers (non-Faradaic). We do not cover these works (Forouzanfar et al., 2020; Ben Aissa et al., 2019; Qureshi et al., 2012; Piccoli et al., 2018), but rather focus our review on sensing mechanisms based on changes in the double layer capacitance.

In the literature of capacitive aptasensors to detect peptides and proteins, there are conflicting, or at least incomplete, mechanistic hypotheses. We will start by discussing capacitive aptasensors targeting thrombin, a large, highly charged blood protein. Thrombin aptamers are unique in that crystal structures of both the RNA and DNA thrombin aptamers have been resolved, which allows observations of the molecular interactions and binding surfaces in the aptamer-thrombin complex. Overlapped crystal structures of the RNA and DNA thrombin aptamers demonstrate that the size of the protein is significantly larger than the folded oligonucleotide structures (Fig. 4a), (Orava et al., 2010) which implies that the contribution to the capacitance changes is dominated by the target rather than the aptamer. With this image of the thrombin aptamer-target complex in mind, we can compare reports of thrombin capacitive aptasensors.

In the work of Chen *et al.,* the capacitive aptasensor demonstrated an *increase* in capacitance in the pM–nM concentration range of thrombin in 1× PBS and 50% serum (Fig. 4b). (Chen et al., 2019) The authors attributed the capacitance increase to the dipole moment of charged thrombin molecules. Given the size of the thrombin dipole and that the study was done at low frequencies (<1 kHz), this hypothesis is reasonable, but it is unlikely a full description of the capacitance change. In contrast, two other works observed the opposite direction of change in the capacitance when sensing thrombin with nanogap (40 nm and 20 nm in respective works) capacitive sensors (Mannoor et al., 2010; Ghobaei Namhil et al., 2019). The data is presented in terms of relative permittivity; this parameter is proportional to capacitance. Both reports show a *decrease* in relative permittivity (*i.e., decrease* in capacitance) upon thrombin target exposure (Fig. 4c). This trend is hypothesized due to the replacement of water molecules (relative permittivity of ~80) by monolayers with lower permittivity (both the aptamers and subsequent thrombin molecules). It should be noted that the physics describing nanoscale electrolytic capacitors is substantially different as both the mean field assumption and electroneutrality of the bulk solution may no longer hold. Two papers, one on charge relaxation (Thakore and Hickman, 2015) and the other on charge fluctuation (Limmer et al., 2013), of nanoscale capacitors give some insight into the unique considerations required at the nanoscale.

While the target molecule and aptamer (albeit there are variations in polyT tail lengths to extend the aptamer from the surface to minimize steric hindrance) are the same between these reports, the difference in the direction of capacitance change demonstrates that the sensor geometry can significantly influence the mechanisms of detection. The disparity in sensor responses also highlights that changes in permittivity for heterogenous substances is not always straightforward and even less so in ionic solutions. Additionally, the use of different buffers likely impacts the measured capacitance.

We now delve into other works where different proteins are targeted with varied hypothesized mechanisms of detection. A capacitive aptasensor based on interdigitated gold electrodes functionalized with an RNA aptamer targeting C-reactive protein (CRP), a critical protein in inflammation and related disorders (Sproston and Ashworth, 2018), demonstrated an *increase* in capacitance upon target capture in two publications from the same group (Qureshi et al., 2010a, 2010b). The authors hypothesized that the larger molecular size of the aptamer-CRP complex leads to a larger permanent dipole moment, which alters

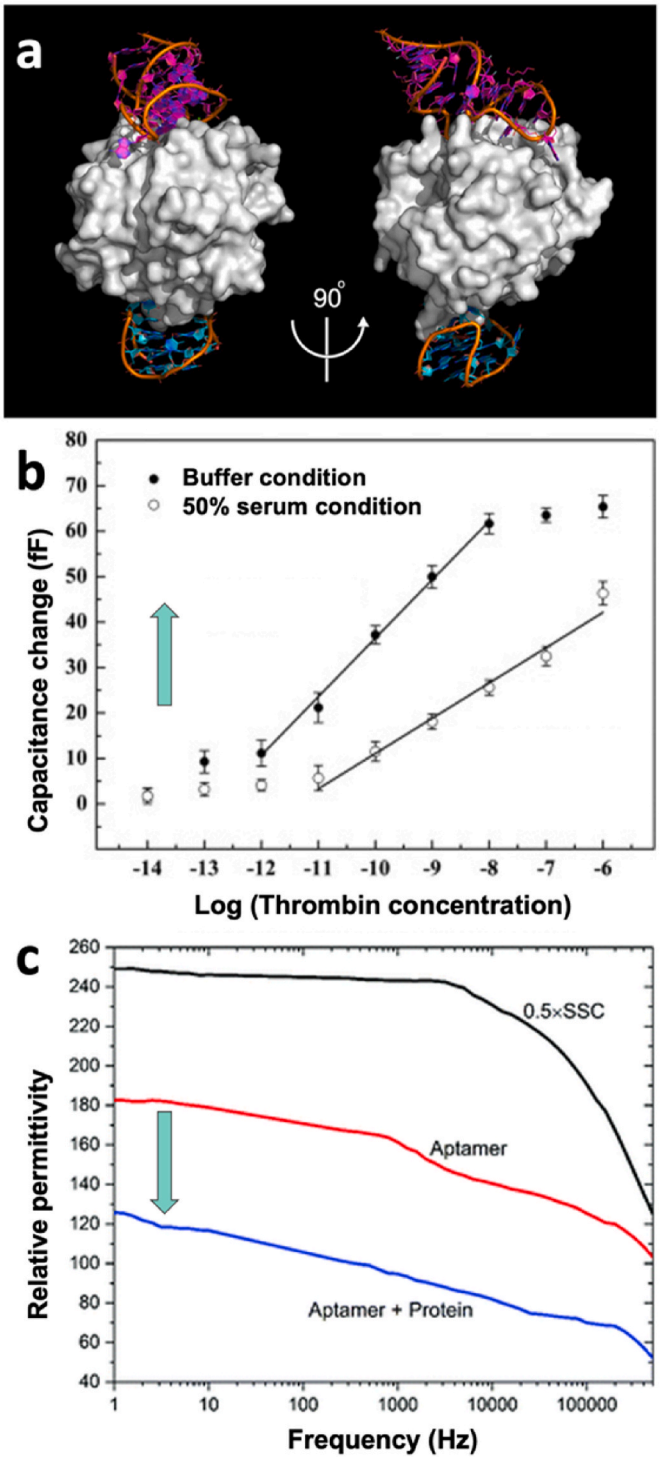

Fig. 4. (a) Overlapped crystal structure of the RNA (purple) and DNA (blue) thrombin aptamer bound to thrombin target (grey), adapted from (Orava et al., 2010), Copyright 2010, with permission from Elsevier. (b) Thrombin detection in buffer (1 × PBS) and 50% serum condition, adapted from (Chen et al., 2019), Copyright 2019, with permission from Elsevier. (c) The relative permittivity *vs.* log (frequency) for a bare nanogap capacitive device in 0.5 × saline-sodium citrate (SSC) buffer (black), after functionalization with thrombin DNA aptamers (red) and upon exposure to 1 μM thrombin target (blue). Adapted from (Ghobaei Namhil et al., 2019), Copyright 2019, with permission from the Royal Society of Chemistry.

dielectric properties of the medium above the electrodes, inducing a change in capacitance. Similarly, Park *et al.* also observed an increase in capacitance upon addition of nicotinamide phosphoribosyltransferase (Nampt), an enzyme in the biosynthesis of nicotinamide adenine dinucleotide, a biomolecule central to metabolism. The malfunction and/or imbalanced concentration of Nampt has been associated with numerous diseases such as cardiovascular diseases (Filippatos et al., 2010) and cancers (Bi and Che, 2010). This change was attributed to the detection of charges present on peripheral amino acids on protein surfaces that are introduced upon interactions with the aptamers.

This work observed an interesting effect – applied frequencies influenced aptamer-target binding (Park et al., 2012). The authors found that the equilibrium constant (K_d) *decreases* (stronger aptamer binding) upon *increasing* the applied AC frequency, resulting in over 100-fold higher target affinities at higher frequencies (~1 GHz). Moreover, an effective frequency range for the dose-dependent response was identified, which is also dependent on the sensing environment (buffers *vs.* complex milieu). While the K_d of the receptors is inherent and unchanging, the authors hypothesized that surface conductance associated with movement of charged protein-bound ions at particular frequencies led to changes in observed binding affinities.

Divergence in capacitance responses was observed from two reports using similar platforms (gold interdigitated microelectrodes) detecting the *same* target molecule: human epidermal growth factor receptor 2 (HER2). The amount of HER2 in blood has been associated with different cancers especially breast cancer (Ludovini et al., 2008). The first HER2 capacitive aptasensor reported in 2015 sensed HER2 using interdigitated 800 × 40 μm electrodes with a spacing of 40 μm with a total sensing surface area of 3 mm^2 and operated in a high frequency region (50–350 MHz, Fig. 5a). (Qureshi et al., 2015) The second HER2 capacitive aptasensor reported in 2018 used 3200 × 5 μm electrodes with 10 μm spacing and a total sensing area of ~15 mm^2, and detected HER2 in a lower frequency range (1–2 Hz, Fig. 5b). (Arya et al., 2018)

In the 2015 sensor, capacitance on the order of pF, *increased* upon exposure to higher concentrations of the target (Fig. 5c). Alternatively, in the 2018 platform, the capacitance in the μF regime, *decreased* with higher HER2 amounts (Fig. 5d). This divergent behavior may be due to various reasons such as the use of different aptamer sequences targeting HER2, varied aptamer functionalization strategies, the different frequency regimes used for target detection, the use of different sample matrices (diluted *vs.* undiluted serum) or blocking agents (bovine serum albumin, BSA *vs.* Tween20). Such variations in experimental conditions despite sensing the same target, render it challenging to associate sensing mechanisms with specific capacitive aptasensor configurations.

In a 2018 paper, a reduction in capacitance was observed with increasing concentrations of *Plasmodium falciparum* glutamate dehydrogenase (PfGDH), a biomarker for malaria diagnosis, both in buffer and whole serum spiked with the analyte (Singh et al., 2018). The authors used a relatively large, 3 mm^2, aptamer functionalized gold disk electrode probed at 2 Hz. The decrease in capacitance was hypothesized to be due to a decrease in the dielectric constant of the double layer upon protein interactions with the aptamer layer. While a valid hypothesis, it neglects the possibility that the changes may be due to differences in the amount of available charge storage withing the double layer after target binding. While the paper includes selectivity measurements by evaluating the sensor response to similar target molecules, the binding curve only showed the linear range, making the reported limit of detection and dynamic range less conclusive.

To conclude this section, it is challenging to correlate capacitive aptasensor responses to specific mechanisms of detection due to the variability in platform, aptamer, target, and experimental design between reports. Evidently, it is necessary to improve our understanding of the contributing effects that drive the measurement readout to gain insight into the optimal design of capacitive aptasensors for specific protein targets of interest.

3.3. Cells

In addition to increasing the thickness of the EDL upon binding to sensing surfaces, cells can play the role of small circuit elements, usually resistors, and thus change the surface impedance/capacitance. Based on this mechanism, most reports indicate a decrease in measured capacitance (*i.e.*, increased impedance). Wu *et al.* adapted their previously reported small-molecule capacitive sensors (BPA and organophosphorus sensors introduced in section 3.1) to detect lipopolysaccharides (LPS) (Wu et al., 2018), a ubiquitously found component in the outer membrane of gram-negative bacteria that can be released during bacterial growth and activate mammalian immune systems (Erridge et al., 2002). Upon LPS recognition, decreased capacitance was recorded and this phenomenon was observed when having free LPS molecules as well as

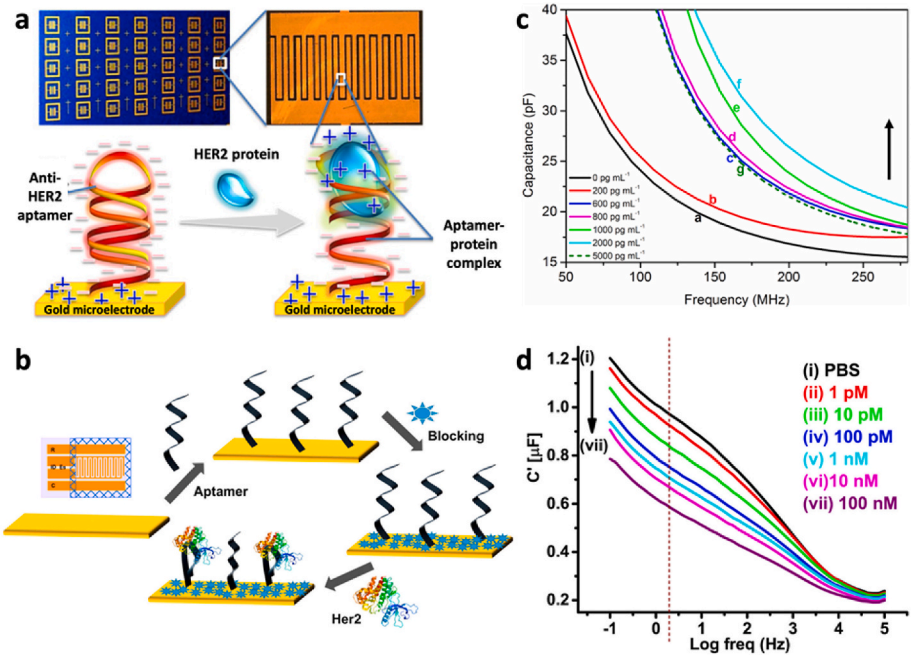

Fig. 5. Divergent behavior observed for two capacitive aptasensors targeting human epidermal growth factor receptor 2 (HER2). (a) Photograph of capacitor array chip (top left) with corresponding microscopic image of interdigitated capacitor (top right). Below, schematics of capacitive chips functionalized with the HER2 aptamer are shown where the DNA backbone contributes negative charges at the capacitor surface. Formation of the aptamer-HER2 complex induces charge distribution and influences the measured capacitance (b) Schematic of the capacitive aptasensor surface chemistry. (c) Capacitance responses showing HER2 target-dependent changes *vs.* frequency sweeps from 50 to 300 MHz. An increase in capacitance was observed except for 5000 pg/mL, hypothesized to arise due to competition between abundant HER2 proteins and limited aptamer binding sites altering the environment. (d) For this aptasensor, a decrease in capacitance was observed in a HER2 concentration-dependent manner. (a) and (c) are adapted from (Qureshi et al., 2015), Copyright 2015, with permission from Elsevier. (b) and (d) are adapted from (Arya et al., 2018), Copyright 2018, with permission from Elsevier.

cell membrane-bound LPS.

Capacitance decreases upon cell recognition were observed in other aptamer-modified capacitive platforms detecting *E. coli*. (Dua et al., 2016) and human lung cancer cell line A549 (Nguyen et al., 2018). Smaller cell derivatives such as exosomes, or extracellular vesicles, also induced a capacitance decrease upon binding to aptamer-modified electrodes. Compared to whole cells an order of magnitude larger in size that modulate the surface capacitance, the signal decrease was attributed to water molecules or ions with a higher dielectric constant compared to the large biomolecules being moved away from the sensing surface upon exosome binding.

Conversely, two articles (Jo et al., 2018; Lee et al., 2020) have reported an *increase* in capacitance when detecting bacterial cells. For example, Jo *et al.* designed a capacitive array for monitoring bacterial growth (Fig. 6a). (Jo et al., 2018) In this aptasensor, upon bacterial growth, capacitance increased (Fig. 6b), and this change was hypothesized to be due to addition of parallel capacitors, *i.e.*, bacteria, to the equivalent circuit. Control measurements were conducted using unmodified bare electrodes and electrodes modified with aptamers not specific to *E. coli*. Even for such large targets (~100 nm ~10 μm), there are varying hypotheses regarding the mechanism of capacitance change upon aptamer recognition.

4. Advancing capacitive aptasensors for clinical relevance

Upon reviewing and analyzing the existing literature of capacitive aptasensing, we now suggest some key aspects that should be considered when translating capacitive aptasensors towards applications with clinical relevance (Fig. 7).

4.1. Optimization of aptamer surface chemistry

To ensure robust immobilization of aptamers on the surface, different approaches are used (Balamurugan et al., 2008) of which two are the most common: well-established gold-thiol chemistry and amide bond formation (Oberhaus et al., 2020). In both cases, incubation time and the concentration of aptamers (White et al., 2008) as well as functionalization condition (*e.g.,* ionic strength and content) (Liu et al., 2021) should be considered to optimize the surface density and ensure reproducibility. While gold-thiol chemistry leads to self-assembly of an aptamer monolayer on the electrode surface without any treatment, for amide bond formation, the surface usually needs to be activated using reagents. Therefore, for the latter, the parameters for the activating conditions (*i.e.,* reaction duration, buffer condition, concentration) should also be optimized.

Further, validation of the surface functionalization is important for every sensing platform despite the use of conventional surface chemistry. For direct detection on sensing surfaces, fluorescence methods can be employed to discern whether homogeneous assembly is achieved. A popular stain to visualize DNA on surfaces is SYBR gold, a highly sensitive dye that shows >1000-fold increase in fluorescence quantum yield upon interacting with DNA (Tuma et al., 1999). Depending on the sensor surface material, quenching effects and auto-fluorescence should be taken into consideration with sufficient calibration and controls.

For surfaces where quenching is an issue, alternative strategies such as monitoring monolayer assembly *in situ* using quartz crystal microbalance with dissipation monitoring (QCM-D) can provide complementary validation of the surface chemistry. This method uses piezoelectric crystals that undergo vibrational oscillations upon application of a voltage (Easley et al., 2022). The changes in frequency and dissipation of the crystal sensor is related to the mass coated on the surface and the viscoelastic properties of the assembled material (Dixon, 2008). Through mathematical modeling, the surface-assembled mass can be converted to changes in layer thickness, which can give insight into the conformational changes aptamers undergo (compression *vs.* elongation of backbone) upon target recognition (Nakatsuka et al., 2021a; Osypova et al., 2015; Belén Serrano-Santos et al., 2012).

Another crucial player in optimizing aptamer surface density is the use of backfillers, small molecules that passivate parts of the electrodes that are exposed to solution and fine tune surface quality. Presence of backfillers usually improves the sensor performance for two reasons: 1) By displacing some of the aptamers, more space is given to remaining aptamers to freely undergo conformational changes to form their functional 3D conformation and/or upon target binding. 2) By passivating the electrode surface, direct nonspecific binding to the electrode is minimized. Although most reports typically use either MCH (Herne and Tarlov, 1997) or ethanolamine based on the surface material, other backfillers for instance with longer length or branches are also available that might be more suitable in some cases (Zhu et al., 2011). When observing the literature, there is high variation in both the backfilling molecule concentration and incubation time. Moreover, some studies co-incubate aptamers and backfilling molecules while others backfill their surface after aptamer functionalization (Herne and Tarlov, 1997).

Alternative to backfilling, one report suggested immobilization of aptamers while they are in target-bound states to ensure leaving enough room for each aptamer to form its functional 3D conformation (Liu et al., 2021). However, this method necessitates strong aptamer-target binding affinities, as the interaction is governed by equilibrium binding kinetics. Thus, a mixture of different aptamer states (bound, unbound, intermediate structures) will likely co-exist in solution when assembling on the surface, which may result in surface density variabilities. The aforementioned factors of surface chemistry and density can significantly affect the reproducibility, sensitivity, and detection range of capacitive aptasensors but are often not been systematically tested and optimized.

4.2. Characterization of aptamer-target interactions

Reviewing the existing literature on capacitive aptasensors demonstrated the importance of correlating observed sensor responses to specific aptamer-target interactions. An in-depth understanding of the possible structural changes in aptamers upon target recognition is especially important when detecting small molecules (Section 3.1). (Bottari et al., 2020) A recent review highlights the need to characterize aptamer-target interactions with multi-analytical approaches, while considering the final application of the aptamer (Daems et al., 2021). Classical analytical methods for studying aptamers (*e.g.,*

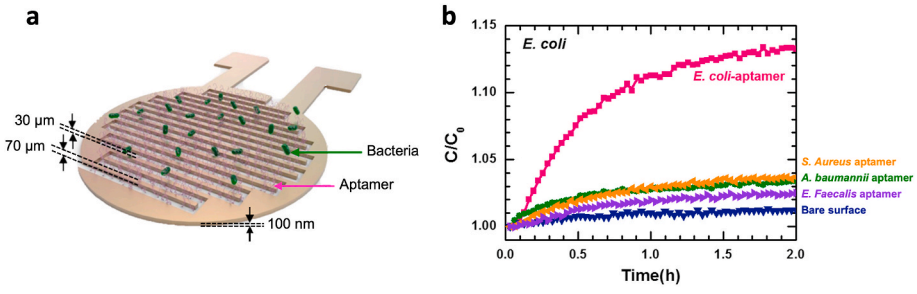

Fig. 6. (a) Schematic of aptamer-functionalized capacitive sensor arrays. DNA aptamers are immobilized on the sensor surface between the electrodes and bacteria are captured by the aptamers, which contributes to an increase in capacitance. (b) Real-time capacitance measured for capacitive arrays functionalized with *Escherichia coli* (*E. coli*) aptamers. Control tests were carried out with either bare unmodified surfaces or electrodes modified with aptamers targeting other bacterial species. Adapted from (Jo et al., 2018), Copyright 2018, with permission from Elsevier.

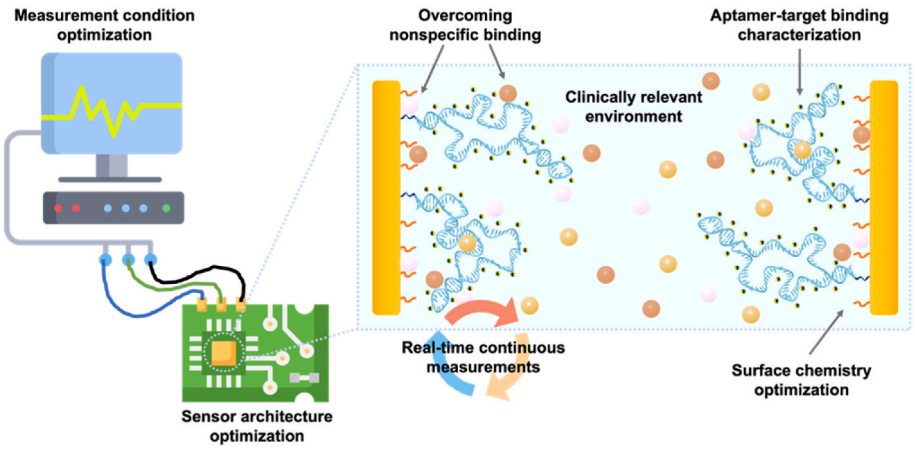

Fig. 7. Key factors that should be considered when translating capacitive aptasensors into clinically relevant sensing platforms.

chromatography approaches and gel-based methods) have been previously reviewed elsewhere (Weaver and Whelan, 2021).

Thermodynamic studies are important for the prediction of sensor kinetics. Label-free solution-based methods such as isothermal titration calorimetry are considered a standard characterization method to determine the binding affinity and reaction stoichiometry between aptamers and their respective targets ranging from small molecules to cells (Challier et al., 2016). Alternatively, native electrospray ionization mass spectrometry not only provides information about the stoichiometry of the aptamer-target binding, but also allows the identification of multiple species co-existing in equilibrium by tracking the mass-to-charge ratio of the aptamer *vs.* target *vs.* aptamer-target complex (Erba and Petosa, 2015). While not as common, fluorescent-based methods can also be employed when the aptamer (*e.g.,* fluorescent nucleobase analogues) (Fadock and Manderville, 2017) or target (*e.g.,* ciprofloxacin) (Jaeger et al., 2019) have intrinsic fluorescent properties.

In addition to thermodynamic studies of aptamer-target interactions, structural methods exist to investigate the conformational changes of aptamers upon target recognition. These methods give insight into the structural motifs (*e.g.,* loops, hairpins, G-quadruplexes, *etc.*) that aptamers adopt both in the free-form and target-bound complex. Circular dichroism spectroscopy is widely used to study aptamer conformations as specific spectra with defined maxima and minima correspond to secondary structural elements (*e.g.,* parallel *vs.* antiparallel G-quadruplex formation) (Kypr et al., 2009; Vorlíčková et al., 2012). Small-angle X-ray scattering is also used as a complementary method to investigate the spatial distribution of electron density on the aptamer (Tomilin et al., 2019). Aptamer structures with atomic resolution can be achieved through nuclear magnetic resonance spectroscopy, X-ray crystallography, and cryo-electron microscopy (Zhang et al., 2021). However, full structural determination at this resolution is highly challenging, which renders these techniques non-trivial for mechanistic investigations.

Since biomolecules free in solution do not necessarily behave the same when tethered to surfaces due to a loss in degree of freedom (Nakatsuka et al., 2018b), surface-based characterization techniques are also powerful ways to mimic the aptamer binding observed at the surface of capacitive sensors. Optical methods such as fluorescence assays, surface plasmon resonance, and surface-enhanced Raman spectroscopy can report binding affinities and kinetics of surface interactions. Depending on the method, the same surface chemistry can be employed as the sensing platform, which better simulates what is happening at the capacitive sensor surface.

Beyond experimental techniques, bioinformatics techniques such as docking programs (Trott and Olson, 2009; Bauke Albada et al., 2015) and computational models including molecular dynamics simulations (Bishop et al., 2007) can predict aptamer structural changes and provide insight into binding sites and intermolecular inteactions with analytes. Recent developments in molecular dynamics simulations have probed the induced-fit mechanism of aptamers undergoing structural rearrangements to bind the target (Lin et al., 2012; Kakoti and Goswami, 2017). In addition to interrogating aptamer-target interactions, simulations combined with machine learning have been extended towards *in silico* rational design and selection of "smart" aptamers with optimal affinities (Douaki et al., 2022). The validation of theoretical models with experimental characterization will significantly improve our understanding of aptamer-target interactions.

4.3. Sensing in clinically relevant environments

When we observe the conditions in which capacitive aptasensors have been tested (Tables 1-3), sensors are often characterized in environments that do not represent the final application medium. Typically, highly diluted buffers (10 to 100-fold), or even water is used. However, capacitive sensors detect changes in relative permittivity and the double layer formed at electrode surfaces, which are influenced by ionic concentrations. Further, aptamer conformational dynamics are strongly influenced by the ionic milieu, thus the sensing environment can heavily influence aptamer-target binding (Nakatsuka et al., 2021b). Sensing in deionized water that lack counterions, impedes highly negatively charged aptamer backbones from adopting thermodynamically stable native secondary structures (Špringer et al., 2010).

Aptamers mimic nature's riboswitches, found mostly in bacteria, where a regulatory element in messenger RNA binds to a small molecule, which triggers changes in transcription. Interactions between riboswitches and small molecules are regulated by environmental cues such as divalent cation concentration (*e.g.,* Mg^{2+}, Ca^{2+}) (Pontes et al., 2016; García Véscovi et al., 1996). This dependence on divalent cations for activity is not limited to riboswitches. DNA-based catalysts (DNAzymes) were reported to cleave RNA based on the presence of Mg^{2+} or Ca^{2+} (Breaker and Joyce, 1995; Faulhammer and Famulok, 1996). Divalent cation-dependent cleavage was shown to be powerful to control the DNAzyme activity as it is compatible with intracellular conditions.

Recently, the influence of divalent cations on dopamine-specific DNA aptamers was also demonstrated (Nakatsuka et al., 2021b), where the presence of Mg^{2+} and Ca^{2+} modulates the magnitude of conformational change upon target recognition. This finding was particularly important since the dopamine aptamer was designed for *in vivo* sensing in the brain microenvironment, where divalent cations are present in mM concentrations. If the dopamine sensor had been tested in water or highly diluted PBS that lacks divalent cations, the high sensitivity achieved in artificial cerebrospinal fluid (that mimics the ionic content of brain fluid) due to the presence of Mg^{2+} and Ca^{2+}, may have been overlooked. To this end, in addition to thorough characterization

Table 1
Summary of reported capacitive aptasensors targeting small molecules.

Target	Sample matrix	Limit of detection	Linear range	Selectivity	Capacitive platform	Applied frequency	Application	Ref.
K^+	Tris buffer solution and pre-treated serum	200 nM	1 μM - 0.1 mM	Na^+, Mg^{2+}, and Ca^{2+}	Three electrode system	–	Environmental and clinical	Kazemi et al. (2015)
Cu^{2+}	0.1 × PBS, tap water, lake water, and soil (all diluted in 0.1 × PBS after required treatments)	2.97 fM	5 fM – 50 pM	Fe^{2+}, Pb^{2+}, As^{3+}, As^{5+}, Hg^{2+}, Mg^{2+}, Al^{3+}, Cr^{3+} and Cr^{6+}	Gold interdigitated electrodes (GID)	1 kHz	Environmental	Qi et al. (2021)
Bisphenol A	0.1 × PBS and canned food diluted in water	109.5 aM	1 fM – 10 pM	Bisphenol S and bisphenol F		500 Hz	Food safety	Mirzajani et al. (2022)
	0.1 × PBS and highly diluted canned foods in water	152.93 aM (calculated)	1 fM – 10 pM			500 Hz		Mirzajani et al. (2017)
	Water, serum, maternal and cord blood (diluted 1:1000 in water)	1 fM	–		Pt interdigitated electrodes	20 kHz	Clinical	Lin et al. (2017a)
	0.1 × PBS	10 fM	1 – 100 fM	Bisphenol S		100 kHz	Environmental	Cui et al. (2016)
	Water and Tris-HCl binding buffer	100 pM	–	–	Anodized aluminum oxide	100 Hz		Kang et al. (2011)
Isocarbophos	0.1 × PBS, 40% profenofos emulsifiable concentrate, and mixture of 20%	0.38 fM	3.46 fM - 3.46 nM	Methamidophos, triazophos, quintozene, and BPA	Al interdigitated electrodes (modified surface acoustic wave (SAW) chips	30 kHz		Zhang et al. (2020)
Profenofos	isocarbophos and 10% triazophos emulsifiable concentrate	0.24 fM	2.68 fM - 2.68 nM					
Omethoate		1.67 fM	4.69 fM - 4.69 nM					
Phorate		0.34 fM	3.84 fM - 3.84 nM					

of aptamer-target interactions, it is important to test the aptamer-modified sensors in buffers that mimic the ionic environment of the final application, and validation should be ultimately conducted in clinically relevant fluids.

4.4. Conducting real-time continuous measurements

In many of the applications mentioned throughout this review, particularly in tracking clinical biomarkers, acquisition of real-time data is indispensable to correlating biomolecule flux with treatments, drug dosage, or disease progression. To date, the goal of deploying real-time electronic biosensors that monitor physiological conditions, directly into clinical settings (akin to the glucose sensor) remains unmet (Liu, 2021). Despite advances in the fields of flexible and stretchable electronics that provide opportunities for interfacing biosensors with specific locations on bodies (Liu et al., 2017), there are additional aspects that hinder translation from the lab to the clinic.

Continuous monitoring necessitates devices with reversible signals that follow the analyte flux while differentiating signals from interferent molecules in complex environments. To track changes in biomarker concentration, the receptor must release the bound target and be regenerated prior to encountering the next analyte. Aptamer-target binding is based on an equilibrium with a characteristic K_d value, which correlates to the affinity of the aptamer to its target. According to equilibrium thermodynamics, the highest sensor sensitivity is expected within an order of magnitude of either side of the K_d value. Thus, to detect low target concentrations, low K_d values (higher binding affinity) are generally preferred.

However, high affinities between aptamers and their targets may render regeneration of the sensor challenging as aptamers will not release bound molecules within appropriate time scales. When aptamer-target binding kinetics are too slow, sensors necessitate external reagents, which hinder continuous measurements. For example, Tran *et al.* reset their capacitive aptasensors using NaOH/NaCl solutions that induce aptamer denaturation for target release (Tran et al., 2011). However, such harsh treatments may not be possible depending on where the sensor is deployed.

Another important parameter in real-time measurements is the required time for the aptamer to the release the target (based on rate constant, k_{off}). This value is critical when high spatiotemporal resolution is needed, *e.g.,* sub-millisecond timescales. Kinetic measurements where bound targets are rinsed *via* medium exchange should be conducted to demonstrate that the sensor can detect targets in a reasonable timescale in specific environments. For instance, while in some capacitive aptasensors, switching back to target-free media did not result in the original baseline capacitance within the experimental timeframe (Kang et al., 2011), alternative electrochemical aptasensors have demonstrated reversible binding in both μM (Swensen et al., 2009) and nM (Erba and Petosa, 2015) regimes.

To the best of our knowledge, there have been no reports of capacitive aptasensors that have conducted real-time measurements in clinically relevant environments. However, reports in which electrochemical (Arroyo-Currás et al., 2017) and transistor-based (Zhao et al., 2021) aptasensors have been successfully used in real-time even *in vivo*, suggest that there is potential to realize clinically relevant capacitive aptasensors by gleaning a fundamental understanding of the aptamer-target binding thermodynamics, kinetics, and sensor readout.

4.5. Determining the optimal capacitive device architecture

Choosing the proper geometry for capacitive aptasensors is not straightforward, as the optimal architecture depends on the target of interest, specific aptamer conformational dynamics, electrode material, production cost of a particular design, and the method used for measuring capacitance. These considerations are not unique to capacitive sensors, rather what is important is having a proper understanding

Table 2
Summary of reported works targeting proteins and peptides.

Target	Sample matrix	Limit of detection	Linear range	Selectivity	Capacitive platform	Applied frequency	Application	Ref.
Thrombin	0.5 × saline sodium citrate buffer	aM (calculated)	–	–	Nanogap (SiO_2 as insulator)	10 – 600k Hz	Clinical	Ghobaei Namhil et al. (2019)
	PBS	1 pM	–	Human serum albumin and BSA	Gold compact disctrode	0.1 Hz – 100k Hz		Chen et al. (2019)
	Mimic serum (coagulated whole blood enriched with proteins)	10 pM	10 pM – 1 μM					
	0.5 × saline sodium citrate buffer	zeptoM (calculated)	–	Lysozyme	Nanogap	10 – 100k Hz		Mannoor et al. (2010)
	0.1 × PBS	267 fM	267 fM – 267 pM	–	MoS_2 nanosheet deposited Pt microelectrode	100 Hz		Lin et al. (2017b)
	1% Serum	53 pM	53 – 854 pM					
CRP	PBS (pH 7.2)	–	100 -500 pg/mL	BSA	GID	50 – 350 MHz		Qureshi et al. (2010a) Qureshi et al. (2010b)
NPY	Artificial CSF	10 ng/mL	10 -1000 ng/mL	–	Three electrode system (Microelectrode)	10 – 5M HZ		López et al. (2021)
Nampt	Tris-binding buffer (100 mM NaCl, 2 mM $MgCl_2$, 5 mM KCl, 1 mM $CaCl_2$, 20 mM Tris and 0.02% Tween 20)	1 ng/mL	1- 50 ng/mL	BSA, vaspin, and retinol binding protein 4	GID	450 – 650 MHz		Park et al. (2012)
	Serum diluted in PBS (1:5)					700M – 1G Hz		
HER2	Diluted serum (10-fold in PBS)	0.2 ng/mL	0.2 - 2 ng/mL	VEGF, EGFR		242 MHz		Qureshi et al. (2015)
	PBS	1 pM	1 pM – 100 nM	PSA, HER4, thrombin		2 Hz		Arya et al. (2018)
	serum					1 Hz		
Ranibizumab	Phosphate buffer (100 mM) pH 5.7 and fermentation broth	8.5 nM	8.5 – 100 nM	GCSF, GOx, urease, and BSA	GID	4.64 Hz	Quality control	Bhardwaj and Jha (2022)
PDGF-BB	Modified PBS (+5 mM $MgCl_2$, pH 7.2)	1 μg/mL	1 - 50 μg/mL	BSA, thrombin, and lysozyme	Three electrode system	5 kHz	Clinical	Liao and Cui (2007)
*Pf*GDH	Binding buffer (50 mM potassium phosphate buffer, 50 mM NaCl, 5 mM KCl, 2.5 mM $MgCl_2$, pH 8.0)	0.43 pM	100 fM – 100 nM	*Pf*-lactate dehydrogenase and -histidine rich protein-II, human- GDH and human serum albumin	Two electrode system	2 Hz		Singh et al. (2018)
	Serum	0.77 pM						
SARS-CoV-2 Nucleocapsid Protein	0.1 × PBS and tap water, serum, plasma, and saliva (all diluted in 0.1 × PBS after required treatments)	3.16, 9.62, 1.82, 2.16, and 1.26 fg/mL respectively	10 fg/mL – 10 pg/mL	Peptidoglycan, PDGF-BB, IgG, human albumin, recombinant spike protein, and histone	Al interdigitated electrodes (modified SAW chips)	100 kHz		Qi et al. (2022)

of the physics and chemistry involved and letting that fundamental insight guide the design. While device architecture is one of the most important parameters in electrical measurements, the relationship between the size of sensing components and optimal target sensing is rarely explored. For instance, while sensor miniaturization leads to a lower physical limit of detection in that each molecule is responsible for a larger percentage change in the capacitance, issues such as diffusion-limited binding, larger noise, increased sensor impedance, and smaller dynamic range can limit the applicability of these sensors. In the reviewed literature, most of the reports used a pre-designed platform without interrogating and verifying whether the dimensions were optimized for the specific target. Electrodes with dimensions of 800 × 40 μm and inter-electrode distances of 40 μm are used in about 15% of studies reported herein (Qureshi et al., 2010a, 2010b, 2015; Park et al., 2012). There is a need to cross-examine the relationship between electrode dimensions such as height, length, width, inter-electrode distance, electrode materials, and electrode configuration with capacitive responses upon target recognition.

Depending on the capacitor dimensions and the applied frequency, the physics involved in sensing the modulation of capacitance will be different. Low frequency modulation, where the applied frequency is much shorter than the characteristic time of ion migration in the capacitor, measures the change of the charge in the double layer. Such measurements are better suited for large surface area electrodes where the impedance of the sensor does not rival that of the instrumentation. However, electrodes with signals averaged across a larger area comes at the expense of the limit of detection. At medium and high frequency modulation, where the applied frequency is on the order of or larger than the characteristic time of ion migration, the measurement is due in part to the dielectric properties of the double layer and potentially the full volume between condenser plates. As the impedance decreases with increasing frequency, smaller capacitors with lower detection limits are enabled. Nevertheless, the system involved should not be diffusion limited and electrochemical noise must be compensated.

4.6. Tackling nonspecific binding by self-referencing

Especially for biosensors with applications in complex environments,

Table 3
Summary of reported works targeting cells.

Target	Sample matrix	Limit of detection	Selectivity	Capacitive platform	Frequency	Application	Ref.
E. coli using LPS	Culture medium diluted in PBS	53 cells/mL	–	GID	100 kHz	Food safety	Wu et al. (2018)
	0.1× PBS	4.9 fg/mL (free LPS)	–				
	0.1× PBS, and spinach sample	4.93 fg/mL (free LPS)	–	Al interdigitated electrodes (modified SAW chips)			Cheng et al. (2019)
	Diluted culture medium (1:100 in water)	267 cells/mL	*S. aureus*				Zhang et al. (2018)
E. coli	Luria broth (cells were washed before experiments)	2 X 10^4 CFU/mL	–	Gap capacitance impedimetric sensor	1 – 1M Hz		Dua et al. (2016)
E. coli using outer membrane protein Ag1	Highly diluted PBS (10^{-6} M)	9 CFU/mL	*Shigella flexneri*	GID	10 kHz	Food safety and environmental	Abdelrasoul et al. (2020)
E. coli, A. baumanii, S. aureus, E. faecalis, ampicillin-resistant *E. coli,* and tetracycline-resistant *E. coli*	Culture medium	10 CFU/mL	*E. coli, A. baumanii, S. aureus, E. faecalis*		1 kHz	Clinical	Jo et al. (2018)
30 clinically relevant strains of *E. coli, A. baumannii, P. aeruginosa, K. pneumoniae, S. aureus* and *E. faecalis*	Mueller Hinton Broth (cation-adjusted)	–	–		1 kHz		Lee et al. (2020)
Lung carcinoma cell line (A549)	Modified PBS (+100 mg/L tRNA + 1 g/L BSA + 5 mM $MgCl_2$ + 4.5 g/L glucose)	1.5 × 10^4 cells/mL	Hela (cervical), MKN45 (gastric), and Caco-2 (colorectal) cancer cell lines and red blood cells	Gold microelectrodes	5 kHz		Nguyen et al. (2018)
Exosomes using CD63	Deionized water	67.84 nM (free CD63)	IgG, Myoglobin, Calnexin, and Bcl-2	Ti/Au interdigitated electrodes (with spots of MoS_s)	1 MHz		Lee et al. (2022)
	Serum	~2200 exosomes/mL					

nonspecific binding is an intrinsic challenge regardless of recognition elements, platform, or design (Frutiger et al., 2021). There are ways to minimize nonspecific binding to the sensor surface by using blocking agents, optimizing surface chemistry, or pre-treating the sample. While selective recognition elements should be chosen to distinguish the target of interest, there is inevitable nonspecific binding – for aptamers that are highly negatively charged, electrostatic interactions are unavoidable.

To circumvent this issue, specific recognition can be discriminated from nonspecific binding by conducting differential measurements. Functionalization of two different areas with specific aptamers *vs.* scrambled sequences (that do not bind the target) enables filtering of the nonspecific signal. The critical factor here, is to ensure that the signal and reference channels have virtually the same degree of nonspecific binding to the surface (equal area, similar chemical signatures of receptors). Further, to reduce the effect of environmental noise, a reduction in distance between the signal and reference channels is important (Frutiger et al., 2021).

5. Conclusions

Aptamer-based biosensors are continuing to grow in popularity due to high specificity, selectivity, stability, relative ease of development, and the various other benefits mentioned above. Diverse transducers have been developed for sensing aptamer-target interactions. In this review, we have covered the literature where capacitive aptasensors were used for measuring different target molecules ranging in size such as small molecules, proteins, and cells. Despite the demonstration of the potential of capacitive aptasensors for the detection of diverse targets, open questions regarding the exact sensing mechanisms, such as the observed direction of change in capacitance, remain unanswered.

Given the diverse explanations for the concept behind capacitive aptasensing, rigorous experiments that test these hypotheses are still necessary to truly advance this field. We have also highlighted key aspects that need to be addressed in future sensor development before capacitive aptasensors would be mature enough for translation outside of the lab. Despite the challenges involved, we believe capacitive aptasensors have the potential to be low cost, label free, parallelizable biosensors that can be used in diverse applications including environmental monitoring, food safety inspection, and clinical diagnostics.

Declaration of competing interest

The authors declare that they have no known competing financial interests or personal relationships that could have appeared to influence the work reported in this paper.

Data availability

No data was used for the research described in the article.

Acknowledgements

The authors thank Prof. Janos Voros for his insightful feedback and helpful discussions. This research was supported by ETH Zürich and the Swiss National Science Foundation.

References

Abdelrasoul, G.N., Anwar, A., MacKay, S., Tamura, M., Shah, M.A., Khasa, D.P., Montgomery, R.R., Ko, A.I., Chen, J., 2020. DNA aptamer-based non-faradaic impedance biosensor for detecting E. Coli. Anal. Chim. Acta 1107, 135–144.

Almeida, S., Raposo, A., Almeida-González, M., Carrascosa, C., 2018. Bisphenol A: food exposure and impact on human health. Compr. Rev. Food Sci. Food Saf. 17 (6), 1503–1517.

Álvarez-Martos, I., Ferapontova, E.E., 2017. A DNA sequence obtained by replacement of the dopamine RNA aptamer bases is not an aptamer. Biochem. Biophys. Res. Commun. 489 (4), 381–385.

Arroyo-Currás, N., Somerson, J., Vieira, P.A., Ploense, K.L., Kippin, T.E., Plaxco, K.W., 2017. Real-time measurement of small molecules directly in awake, ambulatory animals. Proc. Natl. Acad. Sci. U. S. A 114 (4), 645–650.
Arya, S.K., Zhurauski, P., Jolly, P., Batistuti, M.R., Mulato, M., Estrela, P., 2018. Capacitive aptasensor based on interdigitated electrode for breast cancer detection in undiluted human serum. Biosens. Bioelectron. 102, 106–112. November 2017.
Baker, M., 2015. Reproducibility crisis: blame it on the antibodies. Nature 521, 274–276.
Balamurugan, S., Obubuafo, A., Soper, S.A., Spivak, D.A., 2008. Surface immobilization methods for aptamer diagnostic applications. Anal. Bioanal. Chem. 390 (4), 1009–1021.
Bauke Albada, H., Golub, E., Willner, I., 2015. Computational docking simulations of a DNA-aptamer for argininamide and related ligands. J. Comput. Aided Mol. Des. 29 (7), 643–654.
Belén Serrano-Santos, M., Llobet, E., Özalp, V.C., Schäfer, T., 2012. Characterization of structural changes in aptamer films for controlled release nanodevices. Chem. Commun. 48 (81), 10087–10089.
Ben Aissa, S., Mars, A., Catanante, G., Marty, J.L., Raouafi, N., 2019. Design of a redox-active surface for ultrasensitive redox capacitive aptasensing of aflatoxin M1 in milk. Talanta 195 (August 2018), 525–532.
Berggren, C., Bjarnason, B., Johansson, G., 2001. Capacitive biosensors. Electroanalysis 13 (3), 173–180.
Bhardwaj, T., Jha, S.K., 2022. On-line PAT monitoring of lucentis in the fermenter using aptamer-based capacitive microfluidic chip biosensor. J. Electrochem. Soc. 169 (5), 057512.
Bi, T.Q., Che, X.M., 2010. Nampt/PBEF/Visfatin and cancer. Cancer Biol. Ther. 10 (2), 119–125. https://doi.org/10.4161/cbt.10.2.12581.
Bishop, G.R., Ren, J., Polander, B.C., Jeanfreau, B.D., Trent, J.O., Chaires, J.B., 2007. Energetic basis of molecular recognition in a DNA aptamer. Biophys. Chem. 126 (1–3), 165–175.
Bissonnette, S., Del Grosso, E., Simon, A.J., Plaxco, K.W., Ricci, F., Vallée-Bélisle, A., 2020. Optimizing the specificity window of biomolecular receptors using structure-switching and allostery. ACS Sens. 5, 1937–1942.
Bottari, F., Daems, E., De Vries, A.M., Van Wielendaele, P., Trashin, S., Blust, R., Sobott, F., Madder, A., Martins, J.C., De Wael, K., 2020. Do aptamers always bind? The need for a multifaceted analytical approach when demonstrating binding affinity between aptamer and low molecular weight compounds. J. Am. Chem. Soc. 142 (46), 19622–19630.
Breaker, R.R., Joyce, G.F., 1995. A DNA enzyme with Mg^{2+}-dependent RNA phosphoesterase activity. Chem. Biol. 2 (10), 655–660.
Challier, L., Miranda-Castro, R., Barbe, B., Fave, C., Limoges, B., Peyrin, E., Ravelet, C., Fiore, E., Labbé, P., Coche-Guérente, L., Ennifar, E., Bec, G., Dumas, P., Mavré, F., Noë, V., 2016. Multianalytical study of the binding between a small chiral molecule and a DNA aptamer: evidence for asymmetric steric effect upon 3'- versus 5'-end sequence modification. Anal. Chem. 88 (23), 11963–11971.
Chand, R., Han, D., Kim, Y.S., 2016. Rapid detection of protein kinase on capacitive sensing platforms. IEEE Trans. NanoBioscience 15 (8), 843–848.
Chen, Z., Chen, L., Ma, H., Zhou, T., Li, X., 2013. Aptamer biosensor for label-free impedance spectroscopy detection of potassium ion based on DNA G-quadruplex conformation. Biosens. Bioelectron. 48, 108–112.
Chen, H.-J., Chen, R.L.C., Hsieh, B.-C., Hsiao, H.-Y., Kung, Y., Hou, Y.-T., Cheng, T.-J., 2019. Label-free and reagentless capacitive aptasensor for thrombin. Biosens. Bioelectron. 131, 53–59.
Cheng, C., Wu, J., Chen, J., 2019. A highly sensitive aptasensor for on-site detection of lipopolysaccharides in food. Electrophoresis 40 (6), 890–896.
Cui, H., Cheng, C., Lin, X., Wu, J., Chen, J., Eda, S., Yuan, Q., 2016. Rapid and sensitive detection of small biomolecule by capacitive sensing and low field AC electrothermal effect. Sensor. Actuator. B Chem. 226, 245–253.
Daems, E., Moro, G., Campos, R., De Wael, K., 2021. Mapping the gaps in chemical analysis for the characterisation of aptamer-target interactions. TrAC, Trends Anal. Chem. 142, 116311.
Darmostuk, M., Rimpelova, S., Gbelcova, H., Ruml, T., 2015. Current approaches in SELEX: an update to aptamer selection technology. Biotechnol. Adv. 33 (6), 1141–1161.
Dixon, M.C., 2008. Quartz crystal microbalance with dissipation monitoring: enabling real-time characterization of biological materials and their interactions. J. Biomol. Tech. 19 (3), 151–158.
Douaki, A., Garoli, D., Inam, A.K.M.S., Angeli, M.A.C., Cantarella, G., Rocchia, W., Wang, J., Petti, L., Lugli, P., 2022. Smart approach for the design of highly selective aptamer-based biosensors. Biosensors 12 (8).
Dua, P., Ren, S., Lee, S.W., Kim, J.K., Shin, H.S., Jeong, O.C., Kim, S., Lee, D.K., 2016. Cell-SELEX based identification of an RNA aptamer for Escherichia coli and its use in various detection formats. Mol. Cell 39 (11), 807–813.
Easley, A.D., Ma, T., Eneh, C.I., Yun, J., Thakur, R.M., Lutkenhaus, J.L., 2022. A practical guide to quartz crystal microbalance with dissipation monitoring of thin polymer films. J. Polym. Sci. 60 (7), 1090–1107.
Eddleston, M., Buckley, N.A., Eyer, P., Dawson, A.H., 2008. Management of acute organophosphorus pesticide poisoning. Lancet 371 (9612), 597–607.
Ellington, A.D., Szostak, J.W., 1990. *In vitro* selection of RNA molecules that bind specific ligands. Nature 346, 818–822.
Erba, E.B., Petosa, C., 2015. The emerging role of native mass spectrometry in characterizing the structure and dynamics of macromolecular complexes. Protein Sci. 24 (8), 1176–1192.
Erridge, C., Bennett-Guerrero, E., Poxton, I.R., 2002. Structure and function of lipopolysaccharides. Microb. Infect. 4 (8), 837–851.
Fadock, K.L., Manderville, R.A., 2017. DNA aptamer-target binding motif revealed using a fluorescent guanine probe: implications for food toxin detection. ACS Omega 2 (8), 4955–4963.
Faulhammer, D., Famulok, M., 1996. The Ca2+ ion as a cofactor for a novel RNA-cleaving deoxyribozyme. Angew Chem. Int. Ed. Engl. 35 (23–24), 2837–2841.
Filippatos, T.D., Randeva, H.S., Derdemezis, C.S., Elisaf, M.S., Mikhailidis, D.P., 2010. Visfatin/PBEF and atherosclerosis-related diseases. Curr. Vasc. Pharmacol. 8 (1), 12–28.
Fleischmann, S., Mitchell, J.B., Wang, R., Zhan, C., Jiang, D.E., Presser, V., Augustyn, V. Pseudocapacitance, 2020. From fundamental understanding to high power energy storage materials. Chem. Rev. 120 (14), 6738–6782.
Forouzanfar, S., Alam, F., Pala, N., Wang, C., 2020. Highly sensitive label-free electrochemical aptasensors based on photoresist derived carbon for cancer biomarker detection. Biosens. Bioelectron. 170 (September), 112598.
Frutiger, A., Tanno, A., Hwu, S., Tiefenauer, R.F., Vörös, J., Nakatsuka, N., 2021. Nonspecific binding—fundamental concepts and consequences for biosensing applications. Chem. Rev. 121 (13), 8095–8160.
García Véscovi, E., Soncini, F.C., Groisman, E.A., 1996. Mg^{2+} as an extracellular signal: environmental regulation of Salmonella virulence. Cell 84 (1), 165–174.
Ghobaei Namhil, Z., Kemp, C., Verrelli, E., Iles, A., Pamme, N., Adawi, A.M., Kemp, N.T., 2019. A label-free aptamer-based nanogap capacitive biosensor with greatly diminished electrode polarization effects. Phys. Chem. Chem. Phys. 21 (2), 681–691.
Herne, T.M., Tarlov, M.J., 1997. Characterization of DNA probes immobilized on gold surfaces. J. Am. Chem. Soc. 119 (38), 8916–8920.
Jaeger, J., Groher, F., Stamm, J., Spiehl, D., Braun, J., Dörsam, E., Suess, B., 2019. Characterization and inkjet printing of an RNA aptamer for paper-based biosensing of ciprofloxacin. Biosensors 9 (1).
Jo, N., Kim, B., Lee, S.M., Oh, J., Park, I.H., Jin Lim, K., Shin, J.S., Yoo, K.H., 2018. Aptamer-functionalized capacitance sensors for real-time monitoring of bacterial growth and antibiotic susceptibility. Biosens. Bioelectron. 102, 164–170. November 2017.
Kakoti, A., Goswami, P., 2017. Multifaceted analyses of the interactions between human heart type fatty acid binding protein and its specific aptamers. Biochim. Biophys. Acta Gen. Subj. 1861 (1), 3289–3299.
Kang, B., Kim, J.H., Kim, S., Yoo, K.H., 2011. Aptamer-modified anodized aluminum oxide-based capacitive sensor for the detection of bisphenol A. Appl. Phys. Lett. 98 (7).
Kazemi, S.H., Shanehsaz, M., Ghaemmaghami, M., 2015. Non-faradaic electrochemical impedance spectroscopy as a reliable and facile method: determination of the potassium ion concentration using a guanine rich aptasensor. Mater. Sci. Eng. C 52, 151–154.
Kilic, M.S., Bazant, M.Z., Ajdari, A., 2007. Steric effects in the dynamics of electrolytes at large applied voltages. I. Double-layer charging. Phys. Rev. E - Stat. Nonlinear Soft Matter Phys. 75 (2), 1–16.
Kypr, J., Kejnovská, I., Renčiuk, D., Vorlíčková, M., 2009. Circular dichroism and conformational polymorphism of DNA. Nucleic Acids Res. 37 (6), 1713–1725.
Lee, K.S., Lee, S.M., Oh, J., Park, I.H., Song, J.H., Han, M., Yong, D., Lim, K.J., Shin, J.S., Yoo, K.H., 2020. Electrical antimicrobial susceptibility testing based on aptamer-functionalized capacitance sensor array for clinical isolates. Sci. Rep. 10 (1), 1–9.
Lee, M., Park, S.J., Kim, G., Park, C., Lee, M.H., Ahn, J.H., Lee, T., 2022. A pretreatment-free electrical capacitance biosensor for exosome detection in undiluted serum. Biosens. Bioelectron. 199, 113872. December 2021.
Liao, W., Cui, X.T., 2007. Reagentless aptamer based impedance biosensor for monitoring a neuro-inflammatory cytokine PDGF. Biosens. Bioelectron. 23 (2), 218–224.
Limmer, D.T., Merlet, C., Salanne, M., Chandler, D., Madden, P.A., van Roij, R., Rotenberg, B., 2013. Charge fluctuations in nanoscale capacitors. Phys. Rev. Lett. 111 (10), 106102.
Lin, P.-H., Tsai, C.-W., Wu, J.W., Ruaan, R.-C., Chen, W.-Y., 2012. Molecular dynamics simulation of the induced-fit binding process of DNA aptamer and *L*-argininamide. Biotechnol. J. 7 (11), 1367–1375.
Lin, X., Cheng, C., Terry, P., Chen, J., Cui, H., Wu, J., 2017a. Rapid and sensitive detection of bisphenol a from serum matrix. Biosens. Bioelectron. 91, 104–109.
Lin, K.C., Jagannath, B., Muthukumar, S., Prasad, S., 2017b. Sub-picomolar label-free detection of thrombin using electrochemical impedance spectroscopy of aptamer-functionalized MoS_2. Analyst 142 (15), 2770–2780.
Liu, G., 2021. Grand challenges in biosensors and biomolecular electronics. Front. Bioeng. Biotechnol. 9, 1–5.
Liu, Y., Pharr, M., Salvatore, G.A., 2017. Lab-on-Skin: a review of flexible and stretchable electronics for wearable health monitoring. ACS Nano 11 (10), 9614–9635.
Liu, Y., Canoura, J., Alkhamis, O., Xiao, Y., 2021. Immobilization strategies for enhancing sensitivity of electrochemical aptamer-based sensors. ACS Appl. Mater. Interfaces 13 (8), 9491–9499.
López, L., Hernández, N., Reyes Morales, J., Cruz, J., Flores, K., González-Amoretti, J., Rivera, V., Cunci, L., 2021. Measurement of neuropeptide y using aptamer-modified microelectrodes by electrochemical impedance spectroscopy. Anal. Chem. 93 (2), 973–980.
Ludovini, V., Gori, S., Colozza, M., Pistola, L., Rulli, E., Floriani, I., Pacifico, E., Tofanetti, F.R., Sidoni, A., Basurto, C., Rull, A., Crinò, L., 2008. Evaluation of serum HER2 extracellular domain in early breast cancer patients: correlation with clinicopathological parameters and survival. Ann. Oncol. 19 (5), 883–890.
Manning, G.S., 1978. The molecular theory of polyelectrolyte solutions with applications to the electrostatic properties of polynucleotides. Q. Rev. Biophys. 11 (2), 179–246.
Mannoor, M.S., James, T., Ivanov, D.V., Beadling, L., Braunlin, W., 2010. Nanogap dielectric spectroscopy for aptamer-based protein detection. Biophys. J. 98 (4), 724–732.

Mirzajani, H., Cheng, C., Wu, J., Chen, J., Eda, S., Najafi Aghdam, E., Badri Ghavifekr, H., 2017. A highly sensitive and specific capacitive aptasensor for rapid and label-free trace analysis of bisphenol A (BPA) in canned foods. Biosens. Bioelectron. 89, 1059–1067.
Mirzajani, H., Cheng, C., Vafaie, R.H., Wu, J., Chen, J., Eda, S., Aghdam, E.N., Ghavifekr, H.B., 2022. Optimization of ACEK-enhanced, PCB-based biosensor for highly sensitive and rapid detection of bisphenol a in low resource settings. Biosens. Bioelectron. 196, 113745.
Nakatsuka, N., Yang, K.A., Abendroth, J.M., Cheung, K.M., Xu, X., Yang, H., Zhao, C., Zhu, B., Rim, Y.S., Yang, Y., Weiss, P.S., 2018a. Aptamer–field-effect transistors overcome Debye length limitations for small-molecule sensing. Science 362 (6412), 319–324.
Nakatsuka, N., Cao, H.H., Deshayes, S., Melkonian, A.L., Kasko, A.M., Weiss, P.S., Andrews, A.M., 2018b. Aptamer recognition of multiplexed small-molecule-functionalized substrates. ACS Appl. Mater. Interfaces 10 (28), 23490–23500.
Nakatsuka, N., Failletaz, A., Eggemann, D., Forro, C., Voros, J., Momotenko, D., 2021a. Aptamer conformational change enables serotonin biosensing with nanopipettes. Anal. Chem. 93 (8), 4033–4041.
Nakatsuka, N., Abendroth, J.M., Yang, K.A., Andrews, A.M., 2021b. Divalent cation dependence enhances dopamine aptamer biosensing. ACS Appl. Mater. Interfaces 13 (8), 9425–9435.
Nguyen, N.V., Yang, C.H., Liu, C.J., Kuo, C.H., Wu, D.C., Jen, C.P., 2018. An aptamer-based capacitive sensing platform for specific detection of lung carcinoma cells in the microfluidic chip. Biosensors 8 (4).
Ni, S., Yao, H., Wang, L., Lu, J., Jiang, F., Lu, A., Zhang, G., 2017. Chemical modifications of nucleic acid aptamers for therapeutic purposes. Int. J. Mol. Sci. 18 (8), 1683.
Oberhaus, F.V., Frense, D., Beckmann, D., 2020. Immobilization techniques for aptamers on gold electrodes for the electrochemical detection of proteins: a review. Biosens 10 (5), 1–50.
Orava, E.W., Cicmil, N., Gariépy, J., 2010. Delivering cargoes into cancer cells using DNA aptamers targeting internalized surface portals. Biochim. Biophys. Acta Biomembr. 1798 (12), 2190–2200.
Osypova, A., Thakar, D., Dejeu, J., Bonnet, H., Van Der Heyden, A., Dubacheva, G.V., Richter, R.P., Defrancq, E., Spinelli, N., Coche-Guérente, L., Labbé, P., 2015. Sensor based on aptamer folding to detect low-molecular weight analytes. Anal. Chem. 87 (15), 7566–7574.
Park, J.W., Saravan Kallempudi, S., Niazi, J.H., Gurbuz, Y., Youn, B.S., Gu, M.B., 2012. Rapid and sensitive detection of Nampt (PBEF/visfatin) in human serum using an ssDNA aptamer-based capacitive biosensor. Biosens. Bioelectron. 38 (1), 233–238.
Piccoli, J., Hein, R., El-Sagheer, A.H., Brown, T., Cilli, E.M., Bueno, P.R., Davis, J.J., 2018. Redox capacitive assaying of C-reactive protein at a peptide supported aptamer interface. Anal. Chem. 90 (5), 3005–3008.
Pontes, M.H., Yeom, J., Groisman, E.A., 2016. Reducing ribosome biosynthesis promotes translation during low Mg^{2+} stress. Mol. Cell 64 (3), 480–492.
Qi, H., Huang, X., Wu, J., Zhang, J., Wang, F., Qu, H., Zheng, L., 2021. A disposable aptasensor based on a gold-plated coplanar electrode array for on-site and real-time determination of Cu^{2+}. Anal. Chim. Acta 1183, 338991.
Qi, H., Hu, Z., Yang, Z., Zhang, J., Wu, J.J., Cheng, C., Wang, C., Zheng, L., 2022. Capacitive aptasensor coupled with microfluidic enrichment for real-time detection of trace SARS-CoV-2 nucleocapsid protein. Anal. Chem. 94 (6), 2812–2819.
Qureshi, A., Gurbuz, Y., Kallempudi, S., Niazi, J.H., 2010a. Label-free RNA aptamer-based capacitive biosensor for the detection of C-reactive protein. Phys. Chem. Chem. Phys. 12 (32), 9176–9182.
Qureshi, A., Gurbuz, Y., Niazi, J.H., 2010b. Label-free detection of cardiac biomarker using aptamer based capacitive biosensor. Procedia Eng. 5, 828–830.
Qureshi, A., Roci, I., Gurbuz, Y., Niazi, J.H., 2012. An aptamer based competition assay for protein detection using CNT activated gold-interdigitated capacitor arrays. Biosens. Bioelectron. 34 (1), 165–170.
Qureshi, A., Gurbuz, Y., Niazi, J.H., 2015. Label-free capacitance based aptasensor platform for the detection of HER2/ErbB2 cancer biomarker in serum. Sensor. Actuator. B Chem. 220, 1145–1151.
Radi, A.E., O'Sullivan, C.K., 2006. Aptamer conformational switch as sensitive electrochemical biosensor for potassium ion recognition. Chem. Commun. 32, 3432–3234.
Rather, I.A., Koh, W.Y., Paek, W.K., Lim, J., 2017. The sources of chemical contaminants in food and their health implications. Front. Pharmacol. 10 (45), 1–8.
Reverdatto, S., Burz, D.S., Shekhtman, A., 2015. Peptide aptamers: development and applications. Curr. Top. Med. Chem. 15 (12), 1082.
Ricci, F., Vallée-Bélisle, A., Simon, A.J., Porchetta, A., Plaxco, K.W., 2016. Using nature's "tricks" to rationally tune the binding properties of biomolecular receptors. Acc. Chem. Res. 49 (9), 1884–1892.
Santos, A., Piccoli, J.P., Santos-Filho, N.A., Cilli, E.M., Bueno, P.R., 2015. Redox-tagged peptide for capacitive diagnostic assays. Biosens. Bioelectron. 68, 281–287.
Singh, N.K., Arya, S.K., Estrela, P., Goswami, P., 2018. Capacitive malaria aptasensor using Plasmodium falciparum glutamate dehydrogenase as target antigen in undiluted human serum. Biosens. Bioelectron. 117 (June), 246–252.
Špringer, T., Šípová, H., Vaisocherová, H., Štepánek, J., Homola, J., 2010. Shielding effect of monovalent and divalent cations on solid-phase DNA hybridization: surface plasmon resonance biosensor study. Nucleic Acids Res. 38 (20), 7343–7351.
Sproston, N.R., Ashworth, J.J., 2018. Role of C-reactive protein at sites of inflammation and infection. Front. Immunol. 9 (754), 1–11.
Swensen, J.S., Xiao, Y., Ferguson, B.S., Lubin, A.A., Lai, R.Y., Heeger, A.J., Plaxco, K.W., Soh, H.T., 2009. Continuous, real-time monitoring of cocaine in undiluted blood serum *via* a microfluidic, electrochemical aptamer-based sensor. J. Am. Chem. Soc. 131 (12), 4262–4266.
Thakore, V., Hickman, J.J., 2015. Charge relaxation dynamics of an electrolytic nanocapacitor. J. Phys. Chem. C 119 (4), 2121–2132.
Tomilin, F.N., Moryachkov, R., Shchugoreva, I., Zabluda, V.N., Peters, G., Platunov, M., Spiridonova, V., Melnichuk, A., Atrokhova, A., Zamay, S.S., Ovchinnikov, S.G., Zamay, G.S., Sokolov, A., Zamay, T.N., Berezovski, M.V., Kichkailo, A.S., 2019. Four steps for revealing and adjusting the 3D structure of aptamers in solution by small-angle X-ray scattering and computer simulation. Anal. Bioanal. Chem. 411 (25), 6723–6732.
Tran, D.T., Vermeeren, V., Grieten, L., Wenmackers, S., Wagner, P., Pollet, J., Janssen, K. P.F., Michiels, L., Lammertyn, J., 2011. Nanocrystalline diamond impedimetric aptasensor for the label-free detection of human IgE. Biosens. Bioelectron. 26 (6), 2987–2993.
Trott, O., Olson, A.J., 2009. AutoDock Vina:Improving the speed and accuracy of docking with a new scoring function, efficient optimization, and multithreading. J. Comput. Chem. 31 (2), 455–461.
Tsouti, V., Boutopoulos, C., Zergioti, I., Chatzandroulis, S., 2011. Capacitive microsystems for biological sensing. Biosens. Bioelectron. 27 (1), 1–11.
Tuerk, C., Gold, L., 1990. Systematic evolution of ligands by exponential enrichment: RNA ligands to bacteriophage T4 DNA polymerase. Science 249 (4968), 505–510.
Tuma, R.S., Beaudet, M.P., Jin, X., Jones, L.J., Cheung, C.Y., Yue, S., Singer, V.L., 1999. Characterization of SYBR gold nucleic acid gel stain: a dye optimized for use with 300-nm ultraviolet transilluminators. Anal. Biochem. 268 (2), 278–288.
Urmann, K., Walter, J.-G., 2020. Aptamers in Biotechnology.
Vorlíčková, M., Kejnovská, I., Sagi, J., Renčiuk, D., Bednářová, K., Motlová, J., Kypr, J., 2012. Circular dichroism and guanine quadruplexes. Methods 57 (1), 64–75.
Weaver, S.D., Whelan, R.J., 2021. Characterization of DNA aptamer-protein binding using fluorescence anisotropy assays in low-volume, high-efficiency plates. Anal. Methods 13 (10), 1302–1307.
White, R.J., Phares, N., Lubin, A.A., Xiao, Y., Plaxco, K.W., 2008. Optimization of electrochemical aptamer-based sensors via optimization of probe packing density and surface chemistry. Langmuir 24 (18), 10513–10518.
Wu, J., Cheng, C., Yuan, Q., Oueslati, R., Zhang, J., Chen, J., Almeida, R., 2018. Simple, fast and highly sensitive detection of gram-negative bacteria by A novel electrical biosensor. Proc. Annu. Int. Conf. IEEE Eng. Med. Biol. Soc. EMBS 1279–1282.
Yang, K.A., Pei, R., Stefanovic, D., Stojanovic, M.N., 2012. Optimizing cross-reactivity with evolutionary search for sensors. J. Am. Chem. Soc. 134 (3), 1642–1647.
Yang, K.-A., Barbu, M., Halim, M., Pallavi, P., Kim, B., Kolpashchikov, D.M., Pecic, S., Taylor, S., Worgall, T.S., Stojanovic, M.N., 2014. Recognition and sensing of low-epitope targets *via* ternary complexes with oligonucleotides and synthetic receptors. Nat. Chem. 6 (11), 1003–1008.
Yang, K.-A., Chun, H., Zhang, Y., Pecic, S., Nakatsuka, N., Andrews, A.M., Worgall, T.S., Stojanovic, M.N., 2017. High-affinity nucleic-acid-based receptors for steroids. ACS Chem. Biol. 12 (12), 3103–3112.
Yi, M., Jeong, K.H., Lee, L.P., 2005. Theoretical and experimental study towards a nanogap dielectric biosensor. Biosens. Bioelectron. 20 (7), 1320–1326.
Yoon, K., Kwack, S.J., Kim, H.S., Lee, B.M., 2014. Estrogenic endocrine-disrupting chemicals: molecular mechanisms of actions on putative human diseases. J. Toxicol. Environ. Health 17 (3), 127–174.
Zhang, Y., Zhou, H., Ou-Yang, Z.C., 2001. Stretching single-stranded DNA: interplay of electrostatic, base-pairing, and base-pair stacking interactions. Biophys. J. 81 (2), 1133–1143.
Zhang, J., Oueslati, R., Cheng, C., Zhao, L., Chen, J., Almeida, R., Wu, J., 2018. Rapid, highly sensitive detection of gram-negative bacteria with lipopolysaccharide based disposable aptasensor. Biosens. Bioelectron. 112, 48–53.
Zhang, J., Fang, X., Wu, J., Hu, Z., Jiang, Y., Qi, H., Zheng, L., Xuan, X., 2020. An interdigitated microelectrode based aptasensor for real-time and ultratrace detection of four organophosphorus pesticides. Biosens. Bioelectron. 150, 111879.
Zhang, N., Chen, Z., Liu, D., Jiang, H., Zhang, Z.K., Lu, A., Zhang, B.T., Yu, Y., Zhang, G., 2021. Structural biology for the molecular insight between aptamers and target proteins. Int. J. Mol. Sci. 22 (8), 1–27.
Zhao, C., Cheung, K.M., Huang, I.-W., Yang, H., Nakatsuka, N., Liu, W., Cao, Y., Man, T., Weiss, P.S., Monbouquette, H.G., Andrews, A.M., 2021. Implantable aptamer–field-effect transistor neuroprobes for in vivo neurotransmitter monitoring. Sci. Adv. 7 (48), 25–27.
Zhou, J., Rossi, J., 2016 163 2016. Aptamers as targeted therapeutics: current potential and challenges. Nat. Rev. Drug Discov. 16 (3), 181–202.
Zhu, G., Lübbecke, M., Walter, J.G., Stahl, F., Scheper, T., 2011. Characterization of optimal aptamer-microarray binding chemistry and spacer design. Chem. Eng. Technol. 34 (12), 2022–2028.